

RESEARCH ARTICLE

A sturgeon cartilage extracellular matrix-derived bioactive bioink for tissue engineering applications

Xiaolin Meng¹, Zheng Zhou^{2*}, Xin Chen¹, Feng Ren^{3*}, Wenxiang Zhu¹, Shuai Zhu¹, Hairong Liu^{1*}

¹College of Materials Science and Engineering, Hunan University, Changsha 410082, PR China

²College of Biology, Hunan University, Changsha 410082, PR China

³Department of Geriatric Surgery, The Second Xiangya Hospital, Central South University, Changsha, Hunan, 410011, PR China

(This article belongs to the *Special Issue: Advances in 3D bioprinting for regenerative medicine and drug screening*)

Abstract

Three-dimensional (3D) bioprinting provides a promising strategy for tissue and organ engineering, and extracellular matrix (ECM)-derived bioinks greatly facilitate its applications in these areas. Decellularized sturgeon cartilage ECM (dSC-ECM)-derived bioinks for cartilage tissue engineering were fabricated with methacrylate-modified dSC-ECM (dSC-ECMMA) and sericin methacrylate (SerMA), which optimized the mechanical properties of their solidified hydrogels. dSC-ECM induces chondrocytes to form cell clusters and subsequently reduces their proliferation, but the proliferation of encapsulated chondrocytes was normal in solidified dSC-ECM-5 bioink samples, which contain 5 mg/mL dSC-ECMMA. Hence, this bioink was selected for further investigation. Lyophilized dSC-ECM-5 hydrogels showed connected pore microstructure, which is suitable for cell migration and nutrients transportation. This dSC-ECM-5 bioink exhibited high fidelity and good printability by testing via a 3D bioprinting system, and the chondrocytes loaded in printed hydrogel products were viable and able to grow, following incubation, in the cell culture medium. Solidified dSC-ECM-5 and SerMA bioinks loaded with chondrocytes were subcutaneously implanted into nude mice for 4 weeks to test the suitability of the bioink for cartilage tissue engineering. Compared to the SerMA bioink, the dSC-ECM-5 bioink significantly enhanced cartilage tissue regeneration and maturation *in vivo*, suggesting the potential of this bioink to be applied in cartilage tissue engineering in the future.

Keywords: 3D bioprinting; ECM-derived bioink; Cartilage tissue engineering; Cartilage regeneration

*Corresponding authors:

Zheng Zhou
(zhouzheng@hnu.edu.cn)

Feng Ren
(renfeng@csu.edu.cn)

Hairong Liu
(liuhairong@hnu.edu.cn)

Citation: Meng X, Zhou Z, Chen X, *et al.*, 2023, A sturgeon cartilage extracellular matrix-derived bioactive bioink for tissue engineering applications. *Int J Bioprint*, 9(5): 768. <https://doi.org/10.18063/ijb.768>

Received: March 28, 2023

Accepted: April 10, 2023

Published Online: June 6, 2023

Copyright: © 2023 Author(s).

This is an Open Access article distributed under the terms of the Creative Commons Attribution License, permitting distribution, and reproduction in any medium, provided the original work is properly cited.

Publisher's Note: Whioce Publishing remains neutral with regard to jurisdictional claims in published maps and institutional affiliations.

1. Introduction

The applications of 3D bioprinting allow people to manufacture living tissues and organs in the future, and a practicable 3D bioprinting is a collection of science and technologies^[1,2]. Theoretically, tissues and organs are composed of extracellular matrix

(ECM), which is replaced with bioink materials in 3D bioprinting, and living cells. And 3D bioprinting has been achieved with three typical processes, which include designing the models using computer modeling software, slicing the models into smaller pieces, and layer-by-layer printing the models^[3,4]. Hence, functional tissues may be fabricated by precisely assembling bioinks carrying different living cells in a layer-by-layer manner via an appropriate 3D bioprinting machine^[5]. Supported by recent advances in 3D bioprinting technology, the usage of cell-encapsulated biomaterials has been confirmed by researchers as a new approach for cell-based therapeutics and tissue engineering^[6]. However, ECM-derived bioinks have rarely been reported, and different types of ECM-derived bioinks are essential for 3D bioprinting according to various types of cells and their ECM contained in an organ. Bioinks play a key role in 3D bioprinting procedure and its outcome, many of which are capable to solidify and to form a hydrogel structure^[7]. Currently, ECM-derived bioinks are insufficient for 3D bioprinting requirements, and that limits the development of 3D bioprinting applications for tissue printing and tissue and organ engineering^[8-10].

We noticed that the cartilage tissue is consisted of ECM and chondrocytes, and it seems that a proper cartilage ECM-derived bioink and viable chondrocytes are suitable to print hydrogel products for cartilage defects repair and cartilage tissue engineering applications via 3D bioprinting. Since it is difficult to restore cartilage injury naturally by the regeneration ability of patients, implants generated by cartilage tissue engineering or possibly by 3D bioprinting is a feasible approach to resolve severe cartilage defects^[11]. Due to their capacity for chondrocyte induction and similarity to natural cartilage tissue, scaffolds derived from decellularized ECM of native tissues, particularly cartilage, have been confirmed the advantages for cartilage regeneration^[12,13]. ACM (Ac-matrix)-derived hydrogels modified with acrylic anhydride were applied for the regeneration of tracheal cartilage and repair of tracheal circumference^[14]. It is reasonable that decellularized cartilage ECM-derived bioinks may facilitate the application in cartilage defects repair and cartilage tissue engineering.

Cartilage ECM-based scaffolds, which are prepared with cartilage of warm-blooded animals, including bovine, porcine, and caprine, have been proven that they promote cartilage tissue regeneration^[15-18]. However, considering the potential pathogen of those animals that may infect humans, we have fabricated scaffold using decellularized cartilage ECM of sturgeon, a cold-blooded animal. It has been revealed that decellularized sturgeon cartilage ECM (dSC-ECM) is capable of maintaining the

chondrocytic phenotype of chondrocytes^[19]. Furthermore, dSC-ECM scaffolds suppress chondrocyte hypertrophy, which initiates the dedifferentiation of chondrocytes, and facilitates cartilage regeneration^[20]. It has been suggested that human and sturgeon collagen proteins share a high degree of homology, and it has been confirmed by ultra-performance liquid chromatography analysis. Hence, it seems possible that a dSC-ECM-derived bioink may be appropriate for the cartilage tissue engineering applications according to its composition and bioactivity.

In this study, we fabricated three dSC-ECM-derived bioinks and tested their application in cartilage tissue engineering (Figure 1). Those dSC-ECM-derived bioactive bioinks were based on methacrylate-modified dSC-ECM (dSC-ECMMA) and sericin methacrylate (SerMA), which enhanced the mechanical properties of products printed via the 3D bioprinting system. Additionally, a projection-based 3D bioprinter was used to verify whether a selected dSC-ECM-derived bioactive bioink is suitable for 3D bioprinting. Furthermore, printed products encapsulated rabbit chondrocytes were implanted into nude mice to test whether it is able to promote cartilage tissue regeneration and maturation.

2. Materials and methods

2.1. Decellularization of sturgeon cartilage-derived ECM

Decellularized sturgeon cartilage ECM was prepared as the protocol described previously^[20]. In brief, we purchased fresh sturgeons in local markets. Sturgeon cartilage from the fish head was taken out and washed with ddH₂O. The cleaned cartilages were treated for 30 min with 0.1% (v/v) peroxyacetic acid in ddH₂O to kill bacteria and then were washed three times in ddH₂O. Then collected cartilages were cleaned and sliced into small pieces, and these cartilages were frozen in liquid nitrogen for 10 min. They were defrosted at room temperature. The freeze-thaw procedure was performed five times in order to damage the chondrocytes that were already present in these cartilage sections. After 4 h at room temperature, these pieces were treated with 1% sodium lauryl sulfonate (SDS) (Sigma-Aldrich, Poole, UK) solution to change the permeability of cell membrane so that inclusions can permeate selectively and remove cell membrane. Then were washed for three times with ddH₂O.

The cartilage fragments underwent further treatment with 50 U/mL deoxyribonuclease I and 1 U/mL ribonuclease A (Sangon Biotech) for 12 h at 37°C and then washed with ddH₂O for 10 times. For histological analysis, native and decellularized cartilage tissues were preserved with 10% neutral buffered formalin (NBF) for 48h at room

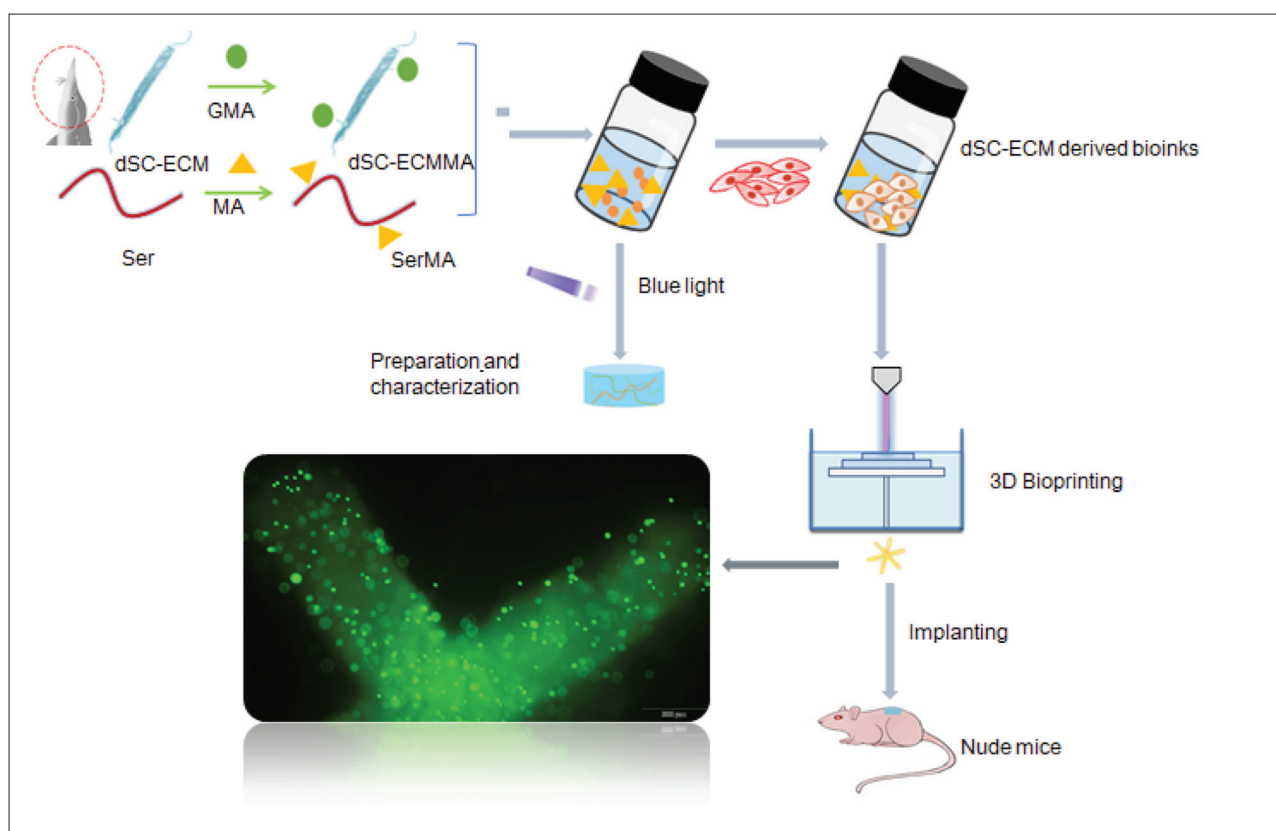


Figure 1. Schematic diagram of preparation and application of the dSC-ECM-derived bioinks as a bioactive bioink for tissue engineering applications. Abbreviations: dSC-ECM, decellularized sturgeon cartilage ECM; dSC-ECMMA, methacrylate-modified dSC-ECM; GMA, glycidyl methacrylate; MA, methacrylate; Ser, sericin; SerMA, sericin methacrylate.

temperature. These samples were paraffin-embedded and cut into 5- μ m sections using a microtome. The sections were deparaffinized and stained with H&E staining for general morphology, safranin-O (SO) staining for GAG and Masson's trichrome (MTS) for collagen. Finally, decellularized cartilage pieces were suspended in ddH₂O and homogenized using a homogenizer (FSH-2A, Yuexin, China) at the speed of 10,000 rpm for 3 min and cooled for 5 min on ice. To obtain the homogenized sturgeon cartilage slurry, the homogenized procedure was carried out twenty times. Finally, slurry-form dSC-ECM was produced. The product was stored at -20°C for further usage.

2.2. Methacrylation of dSC-ECM

For methacrylation, 0.5 g of dSC-ECM was resuspended in 100 mL of PBS with stirring at 1000 rpm for 2 h at 25°C . Then, 0.4 mL of glycidyl methacrylate (GMA) (Sigma-Aldrich, St. Louis, USA) was mixed into this dSC-ECM-containing solution with stirring at 1000 rpm for 12 h at 25°C . The resulted solution was dialyzed against distilled water using a dialysis membrane (MWCO 3500 Da) for 7 days. After centrifugation, the bottom precipitate was freeze-dried to obtain the dSC-ECMMA. Finally, sponge-

form dSC-ECMMA powder was produced. The product was stored at -20°C for further usage.

2.3. Synthesis of SerMA

The SerMA preparation was carried out according to the protocol described in the publication^[21]. In brief, sericin (5.0 g) was dissolved in 20 mL PBS (pH 8.5) at 35°C for 2 h. Following that, dropwise additions of methacrylic anhydride (4 mL) in PBS (50 mL) were made to the sericin solution. Finally, products of reaction were dialyzed and lyophilized, and then SerMA powders were produced. Obtained SerMA powders were stored at 4°C for further usage.

2.4. The formulation of dSC-ECM-derived bioinks

Since dSC-ECMMA is not dissolved in water, an additional ingredient may be added to compose a photo-curing bioink. Transparent ear molds were used to test the ability of photocrosslinking and handling of bioinks composed with different formulations.

To compose photo-curable bioinks, a series of dSC-ECM-derived bioinks precursor solutions were prepared, which contained 5 mg/mL LAP, 150 mg/mL SerMA, and

5 mg, 10 mg, and 15 mg/mL dSC-ECMMA, respectively, which were correspondingly defined as dSC-ECM-5, dSC-ECM-10, and dSC-ECM-15. A bioink precursor solution containing 150 mg/mL SerMA and 5 mg/mL LAP only was prepared as the control bioink sample. Finally, those samples were solidified by exposure to blue light (wavelength: 405 nm) to test their ability to photocuring and operability for further cell culture. Hydrogel samples prepared from the dSC-ECMMA containing bioink precursor solutions are simply described as dSC-ECM-5, dSC-ECM-10, and dSC-ECM-15 hydrogels, respectively, in later statements.

2.5. Characterizations of hydrogels prepared with dSC-ECM-derived and the control bioinks

2.5.1. ^1H NMR tests

The key component of bioinks, dSC-ECMMA and SerMA, were characterized and compared with proton nuclear magnetic resonance (^1H NMR) measurements. For the ^1H NMR analysis, 10 mg of SerMA were completely dissolved in 1 mL of deuterium oxide (D_2O ; Sigma-Aldrich, St. Louis, USA). The dSC-ECM and dSC-ECMMA samples were dissolved as much as possible in D_2O . All samples in D_2O were analyzed by ^1H NMR (Bruker 400 MHz Advance, Switzerland) to obtain a corresponding NMR spectrum.

2.5.2. Rheological properties

Rheological properties of dSC-ECM hydrogels and SerMA hydrogel were evaluated using a rheometer (MCR 92, Anton Paar GmbH) with oscillation frequency from 1 to 10 Hz. The cylinder samples, which were 0.3 mm in height and 15 mm in diameter cylinder shape, were prepared for the rheological properties test.

2.5.3. Mechanical properties tests

The mechanical properties of hydrogel samples were measured using the electronic universal testing machine (AGS-V universal testing machine with a 20 N sensor, Shimadzu Corporation). As-prepared cylindrical hydrogel samples ($d = 10$ mm, $h = 3$ mm) were placed at the center of the horizontal measuring platform. All tests were done on 3 samples ($n=3$).

2.5.4. Equilibrium swelling ratio

The swelling behavior of dSC-ECMMA hydrogels and SerMA hydrogels was measured via the gravimetric method. Briefly, samples were immersed for 0.125, 0.5, 1, and 1.5 h in $1\times$ PBS (pH 7.4) at 37°C . The hydrogels were washed three times with ddH_2O , and the filter paper was used to blot the surface liquid of the hydrogel as much as possible. The hydrogels were weighed at the different time points described above to obtain W_{swollen} . Then the gels were lyophilized and measured the dried weight (W_{dry}). The ratio of water uptake from dried dSC-ECMMA hydrogels

and SerMA hydrogel (Q) can be calculated as the following formulation:

$$Q = (W_{\text{swollen}} - W_{\text{dry}}) / W_{\text{dry}} \times 100(\%) \quad (\text{I})$$

2.6. Isolation and cultivation of rabbit chondrocytes

All animal experiments in this research were approved by the Animal Care and Ethics Committee of College of Biology, Hunan University. The isolation and culture of rabbit chondrocytes followed the protocol described in the publication without any modification^[22]. Chondrocytes in the second passage were harvested for further experiments.

2.7. Cytocompatibility of dSC-ECM hydrogels

AlamarBlue assays and fluorescein diacetate (FDA) staining were carried out to evaluate the cytocompatibility of prepared hydrogel samples, which encapsulated living chondrocytes. SerMA hydrogels, which were prepared by photocrosslinking SerMA bioink precursor solution carrying chondrocytes (10×10^5 cells/mL), were used as the control samples. The dSC-ECM hydrogel samples were produced by irradiating dSC-ECM-derived bioinks (10×10^5 chondrocytes/mL), which contained 5, 10, and 15 mg/mL dSC-ECMMA, respectively (described at 2.4), with blue light. Then, these samples with encapsulated chondrocytes were transferred to cell culture plates with high glucose DMEM containing 10% FBS. The cell culture plates with samples were incubated in a humidified 37°C , 5% CO_2 incubator. In brief, the cell-loaded hydrogel samples incubated for 1 and 7 days were taken out, stained with FDA, and observed with an inverted fluorescent microscope (IX-73, Olympus, Japan). The cellular proliferation was analyzed following 1 and 5 days of incubation using the AlamarBlueTM Assay kit (Thermo Fisher Scientific). Briefly, all samples were washed three times with PBS and incubated in a fresh medium containing 10% v/v AlamarBlueTM dye solution at 37°C . After 6 h incubation, 200 μL of the medium was collected and measured the fluorescence with excitation at 570 nm and emission at 630 nm with a spectrophotometer (Thermo Multiskan MK3, USA).

2.8. Scanning electron microscopy and porosity measurement of lyophilized dSC-ECM-5 and SerMA hydrogels

The microscopic morphology of samples, which were lyophilized dSC-ECM-5 and SerMA hydrogels, were observed by scanning electron microscope (SEM) at an accelerating voltage of 30 kV (FEI Quanta 200, FEI Company, Czech Republic). The average pore sizes of the lyophilized hydrogels were analyzed from the SEM images by using ImageJ (50 random pores for each sample were calculated).

Table 1. The parameters of 3D printing

Thickness (μm)	Section numbers (400 μm /layer)	Exposure time per layer (s)	Exposure intensity (mWcm^{-2})
1600	4	30	18

Table 2. The sequence of primers used for RT-qPCR

Full name of each RNA	Abbreviation	5'–3'	Primer sequences
Glyceraldehyde-3-phosphate	GAPDH	Forward Reverse	TTGTCGCCATCAATGATCCAT GATGACCAGCTTCCCGTTCTC
SRY-related HMG box 9	SOX9	Forward Reverse	GCGTCAACGGCTCCAGCAAGA GCGTTGTGCAGGTGCGGGTAC
Aggrecan	AGG	Forward Reverse	GCTGCTACGGAGACAAGGATG CGTTGCGTAAAAGACCTCACC
Type II collagen	COL II	Forward Reverse	GAGAGCCTGGGACCCCTGGAA CGCCTCCAGCCTTCTCGTCAA
Type I collagen	COL I	Forward Reverse	CTAGCCACCTGCCAGTCTTTA GGACCATCATCACCATCTCTG

2.9. Bioprinting application of dSC-ECM-5 derived bioink

The dSC-ECM-5-derived bioink with the concentration of 5 mg/mL dSC-ECMMA was prepared as described above, and the SerMA bioink instead of dSC-ECMMA was applied as a control. All tested bioink samples carried chondrocytes at a density of 10×10^6 cells/mL. The dSC-ECM-5 solution containing chondrocytes was then added to the 3D printing system's loading tank and printed one layer at a time to create the designed shape. Table 1 displays the 3D printing process parameters. Following printing, the variously shaped cell-loaded hydrogel products were obtained and observed using a digital microscope (Dino-Lite, ANMO ELECTRONICS Corporation). Living cells of the test samples were observed using an inverted fluorescent microscope (IX73, Olympus, Japan) following FDA staining after 7 days of culture.

2.10. RNA isolation and real-time quantitative polymerase chain reaction analysis

The influence of dSC-ECM-5 on the transcription of chondrocytes was examined by real-time quantitative polymerase chain reaction (RT-qPCR) assays (Table 2). Chondrocytes encapsulated in dSC-ECM-5 and SerMA hydrogels were respectively cultured *in vitro* for 2 weeks, and the total RNA was isolated from tested samples to measure the transcription level of genes related to chondrogenesis. The isolation of total RNA and RT-qPCR assay was performed according to our publication^[22]. In brief, trace DNA contamination of RNA samples was removed by DNase I after total RNA of chondrocytes was extracted by lysing in TRIzol (Invitrogen, USA) (Fermentas, Canada). The PrimeScript Reverse Transcriptase (TakaRa,

Japan) was then used to reverse transcribe these RNA samples to create complementary DNA. The RT-qPCR test was utilized to analyze the samples, and the gene of glyceraldehyde-3-phosphate dehydrogenase (GAPDH) was used as the control. Ultra SYBR mixture used in the RT-qPCR assays was acquired from CWBIO (China). The primers of the test genes for RT-qPCR were designed by Oligo software and their sequence was validated by BLAST on NCBI website.

2.11. Test of dSC-ECM-5-derived bioink for tissue engineering applications

Applying dSC-ECM-5-derived bioink to cartilage tissue regeneration *in vivo* was investigated by subcutaneous implanting printed hydrogel products with encapsulated chondrocytes in nude mice, which were acquired from Hunan Slake Jingda Experimental Animal Co., Ltd (male, 6–8 weeks old, 18–20 g/mice). Prepared chondrocytes-loaded dSC-ECM-5 hydrogel samples were cultured *in vitro* for 3 days and then implanted under the skin of nude mice. After implantation, nude mice were kept in two cages and given distilled water and food. Then, they were allowed to move freely in cages. Nude mice were sacrificed after surgery for 4 weeks and specimens were collected and subjected to the H&E, SO, and type II collagen immunohistochemical staining. And stained specimens were observed by a microscope to evaluate their *in vivo* cartilage tissue regeneration efficiency.

2.12. Data analysis

GraphPad Prism 7.00 was used for statistical computing and graph preparation. All data are expressed as mean \pm standard deviation for a minimum of $n=3$. Significant

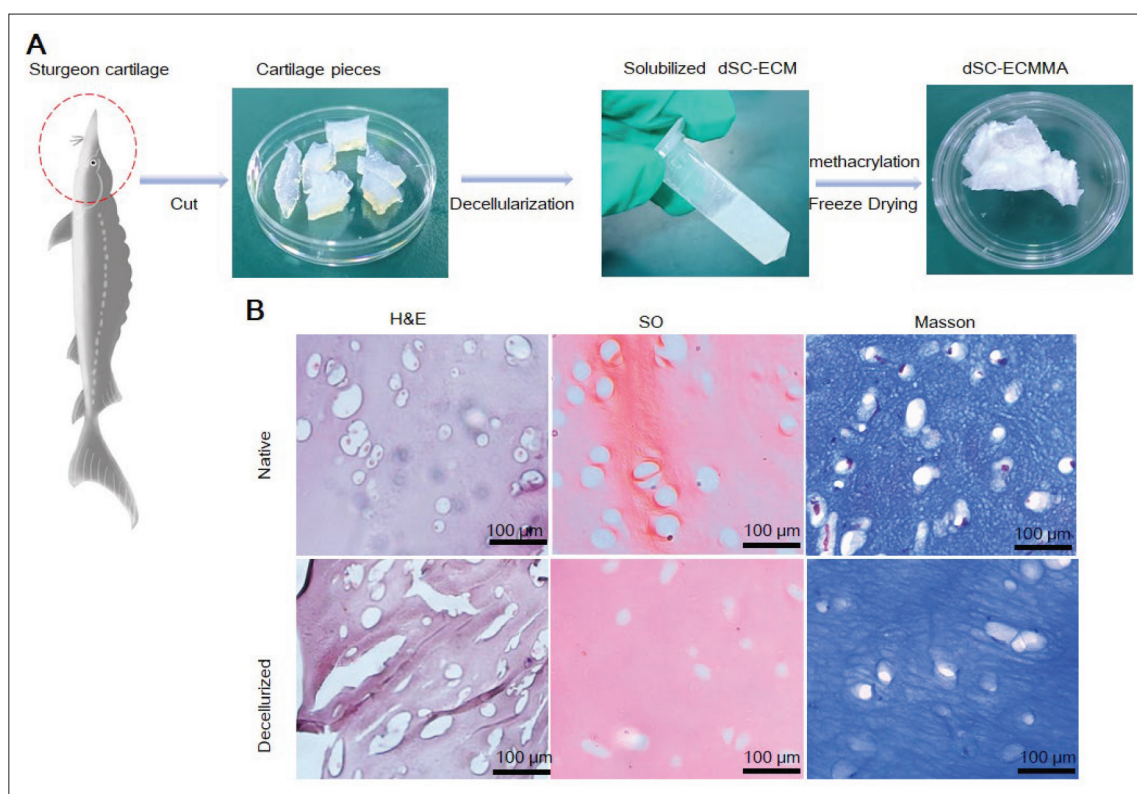


Figure 2. Preparation and characterization of methacrylate-modified decellularized sturgeon cartilage ECM (dSC-ECMMA). (A) Preparation of dSC-ECM by decellularization and methacrylate-modified procedures; (B) histological analyses of native and decellularized sturgeon cartilage ECM by H&E, SO, and Masson. Abbreviations: H&E, hematoxylin and eosin; Masson, Masson's trichrome; SO, safranin-O.

differences between groups were calculated by one-way analysis of variance (ANOVA) at a confidence interval of 95% via GraphPad Prism 7.00 software. The differences were considered significant at $p < 0.05$ (*), $p < 0.01$ (**), and $p < 0.001$ (***)

3. Results

3.1. Characterization of dSC-ECM hydrogel samples

It has been suggested that the advantages of decellularization include maximal clearance of cellular and genetic molecules and minimal loss of ECM components. Decellularized cartilage extracellular matrix (Dc-ECM) seems to be an ideal natural material with bioactivity for cartilage tissue regeneration compared with synthetic biomaterials. In this study, sturgeon cartilage was prepared into dSC-ECMMA by the procedures including tissue preparation, decellularization, solubilization, and methacrylation (Figure 2A). Decellularized sturgeon cartilage fragments and sturgeon cartilage tissues were sectioned and evaluated using HE and SO staining, confirming the elimination of cellular and genetic molecules. No positive cell nuclei image was observed in decellularized sturgeon cartilage fragments after a series of decellularization procedures, showing that

the decellularization process effectively eliminated resident chondrocytes (Figure 2B). However, obtained dSC-ECM required further modification, by which it could crosslink with other components of bioinks and solidify into hydrogel during 3D bioprinting procedure^[23]. To achieve this purpose, methacrylate (MA) was used to modify dSC-ECM and generated methacrylate-modified dSC-ECM (dSC-ECMMA) particles, which were theoretically photocurable and capable of photo crosslinking. After 10 s of blue light (405 nm, 10 mW/cm²) exposure, the dSC-ECMMA solutions transformed to crosslinked hydrogels.

To confirm the methacrylation of dSC-ECM and sericin, ¹H NMR spectra tests were made to assess the prepared samples. According to the results of ¹H NMR spectra, it confirmed that MA was successfully conjugated onto sericin as the new peaks occur at "C=C" (δ 5.6 ppm and 6.1 ppm) and "-CH₃" (δ 1.8 ppm). Furthermore, these ¹H NMR spectra results displayed that MA was successfully conjugated onto dSC-ECM as the new peaks occur at "C=C" (δ 5.7 ppm and 6.2 ppm) and "-CH₃" (δ 1.8 ppm). Hence, the C=C bond was introduced to the dSC-ECM and sericin respectively, by grafting MA to them and obtaining photocurable dSC-ECMMA and SerMA (Figure 3A).

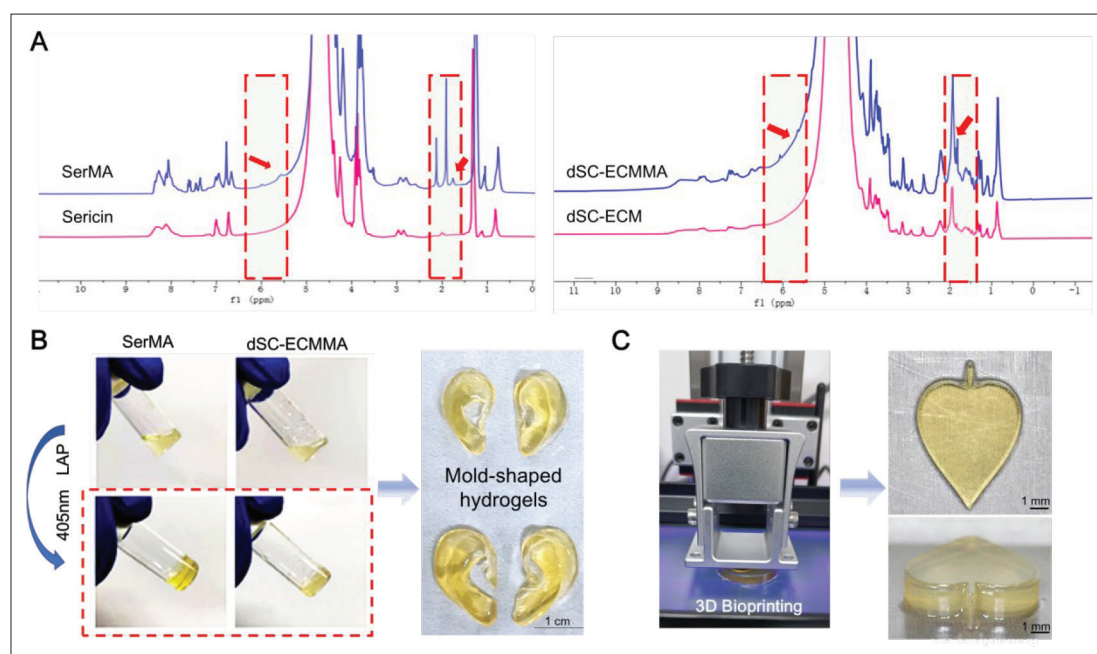


Figure 3. The photocrosslinking process of dSC-ECMMA hydrogels. (A) ¹H NMR spectra of SerMA, dSC-ECMMA (the red arrows indicate the methacrylamide group signal peaks). (B) The photocrosslinking process. (C) The bioprinting process of constructs based on dSC-ECMMA. Abbreviations: ¹H NMR, proton nuclear magnetic resonance; dSC-ECMMA, methacrylate-modified dSC-ECM; SerMA, sericin methacrylate.

3.2. Physicochemical properties of dSC-ECM hydrogels

Since dSC-ECMMA is not totally water soluble, the dSC-ECM-derived bioinks were consisted of dSC-ECMMA and SerMA, which were added to optimize the mechanical properties of their solidified hydrogels. The elastic modulus of SerMA hydrogels is 200 kPa, and that of dSC-ECM hydrogels increased from 200 to 400 kPa resulting from the incorporation of dSC-ECM (Figure 4A and B).

The liquid absorption swelling rate of the dSC-ECM and SerMA hydrogels were comparable and over 400% (Figure 4C), showing that all samples are well suited to the moist environment of synovial joints and are capable to store nutrients in liquid environments effectively^[24].

An oscillatory rheological measurement was employed to describe the rheological characteristics of the dSC-ECM and SerMA hydrogels, and the data illustrated that these hydrogels were viscoelastic resulting from their storage modulus (G') was higher than their loss modulus (G'') (Figure 4D and E). In summary, photo crosslinked dSC-ECM hydrogel displayed high porosity, good viscoelasticity, and reliable mechanical strength, which are suitable for tissue engineering applications. Hence, a series of dSC-ECM-derived bioinks, which contained 5 mg/mL, 10 mg/mL, and 15 mg/mL dSC-ECMMA besides SerMA, were prepared and named as dSC-ECM-5, dSC-ECM-10, and dSC-ECM-15, respectively.

3.3. Biocompatibility of solidified hydrogels prepared with dSC-ECM-derived bioinks

It is crucial to assess their biocompatibility *in vitro* before using crosslinked bioinks for tissue engineering applications *in vivo*^[24]. To determine whether the hydrogels prepared with dSC-ECM-derived bioinks facilitate the cell viability and the cellular proliferation, prepared hydrogel samples, which contained 5 mg/mL (dSC-ECM-5), 10 mg/mL (dSC-ECM-10), and 15 mg/mL dSC-ECMMA (dSC-ECM-15) respectively, with encapsulated chondrocytes were incubated with cell culture medium. The proliferation of chondrocytes in all samples was examined by FDA staining following 1, 3, 5, and 7 days of incubation (Figure 5A). The growth of chondrocytes was observed only in the samples which containing 5 mg/mL dSC-ECMMA compared with the SerMA samples, indicating that only the dSC-ECM-5 bioink is suitable for tissue engineering applications. To further confirm this observation, hydrogel samples prepared with dSC-ECM-5 and SerMA bioinks were respectively incubated with cell culture medium. Following 1, 3, and 5 days of incubation, the proliferation of encapsulated chondrocytes was measured with AlamarBlue assays (Figure 5B). It exhibited that the proliferation of chondrocytes in dSC-ECM-5 samples was similar to that in SerMA samples. Hence, the dSC-ECM-derived bioink, dSC-ECM-5, is fit for tissue engineering applications due to its good biocompatibility and selected for further testing.

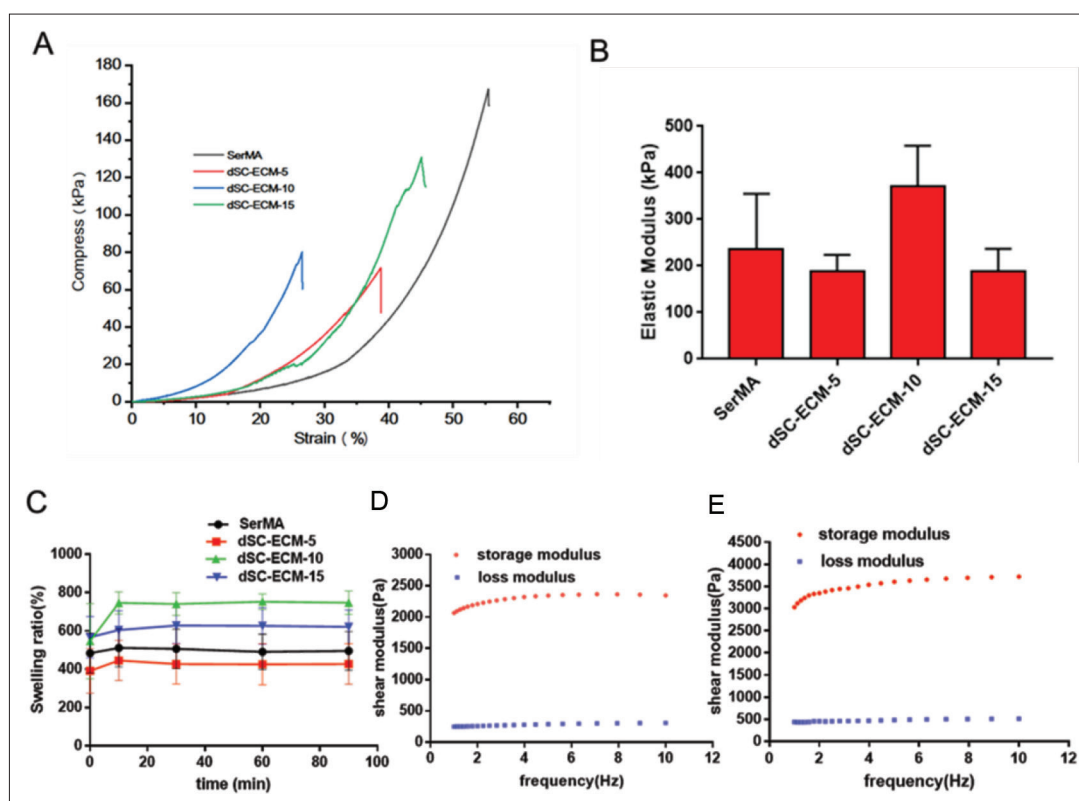


Figure 4. Characterization of dSC-ECM and SerMA hydrogel. (A) The compressive curves. (B) Elastic modulus (kPa). (C) Swelling rate. (D) Rheological properties of SerMA hydrogel. (E) Rheological properties of dSC-ECM hydrogel. Abbreviations: dSC-ECM, decellularized sturgeon cartilage ECM; SerMa, sericin methacrylate.

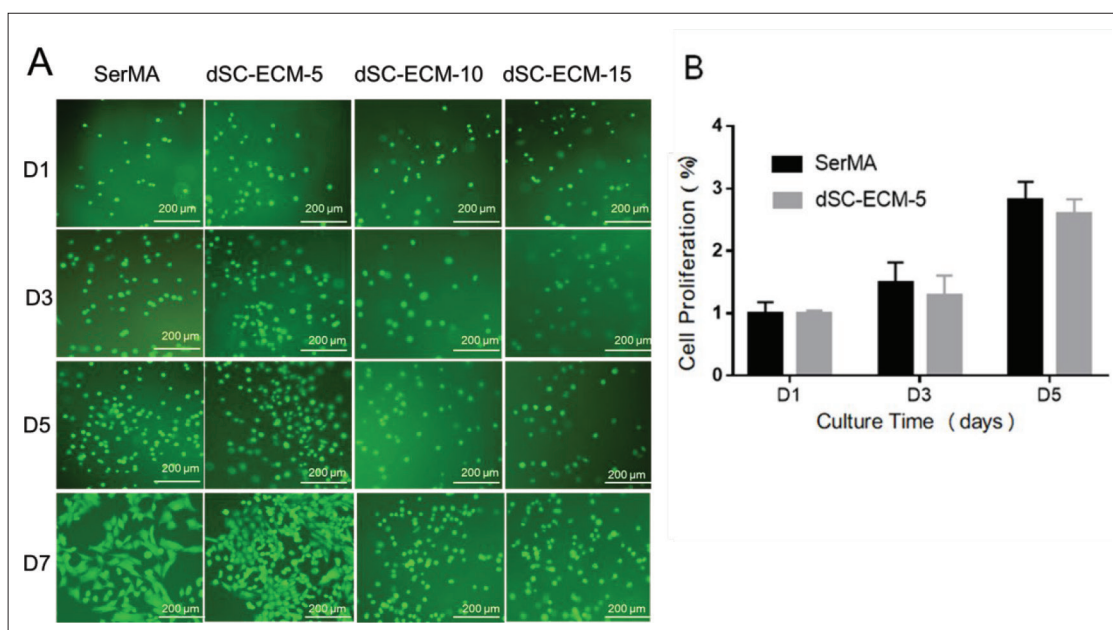


Figure 5. (A) Cell proliferation of chondrocytes encapsulated in hydrogel samples prepared with dSC-ECM-5, dSC-ECM-10, dSC-ECM-15, and SerMA bioinks *in situ* after 1, 3, 5, and 7 days of incubation, respectively. (B) Proliferation rate of rabbit chondrocytes loaded in hydrogel samples solidified with dSC-ECM-5 and SerMA bioinks. Abbreviations: dSC-ECM-5, 5 mg dSC-ECMMA; dSC-ECM-10, 10 mg dSC-ECMMA; dSC-ECM-15, 15 mg/mL dSC-ECMMA; SerMa, sericin methacrylate.

3.4. The microstructure of dSC-ECM-5 hydrogels

The microstructure of lyophilized dSC-ECM-5 and SerMA hydrogels were characterized by SEM (Figure 6A). It demonstrated that both lyophilized dSC-ECM-5 and SerMA hydrogels exhibited a similar porous network structure. Pore sizes of lyophilized dSC-ECM-5 hydrogels were mainly

distributed between 50 and 100 μm , and connected pore size of lyophilized SerMA hydrogels was distributed from 30 to 60 μm (Figure 6B). It indicated that the connected pores of dSC-ECM-5 and SerMA hydrogels were available for effective material transport and signal transmission, which are crucial for tissue engineering applications.

3.5. The dSC-ECM-5 bioink for 3D bioprinting applications

By employing 3D bioprinting, a more advanced 3D printing technique, hydrogel products with designed shapes and containing active cells in a suitable microenvironment can be manufactured and greatly facilitate tissue engineering applications^[25,26]. Strategies for tissue engineering have been reenergized by the potential of 3D bioprinting techniques, which not only achieve the accurate distribution of biomaterials and cells but also acquire the individual customization of specific shapes^[27]. The projection-based 3D printer was selected as a 3D bioprinting machine. The dSC-ECM-5 bioink with the cell density of 1×10^6 chondrocytes/mL was used as the raw material for 3D printer, and optimized printing parameters (Table 1) were obtained after three preliminary trials. Subsequently, the dSC-ECM-5 bioink carrying chondrocytes was printed into hydrogel products with designed shapes by using optimized parameters via this 3D printer (Figure 7). Following bioprinting, it demonstrated that the produced shapes were high fidelity and clearly delineated, suggesting that dSC-ECM-5 is a promising bioink for 3D bioprinting. Then these hydrogel samples printed with the dSC-ECM-5 bioink were transferred

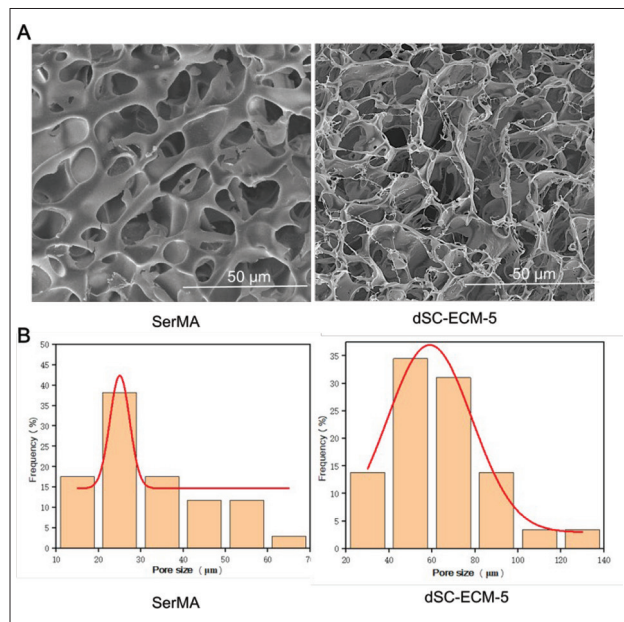


Figure 6. Characterization of dSC-ECM-5 and SerMA hydrogel. (A) SEM of lyophilized dSC-ECM-5 and SerMA hydrogel. (B) Pore size distribution of lyophilized hydrogels. Abbreviations: dSC-ECM-5, 5 mg dSC-ECMMA; SerMA, sericin methacrylate.

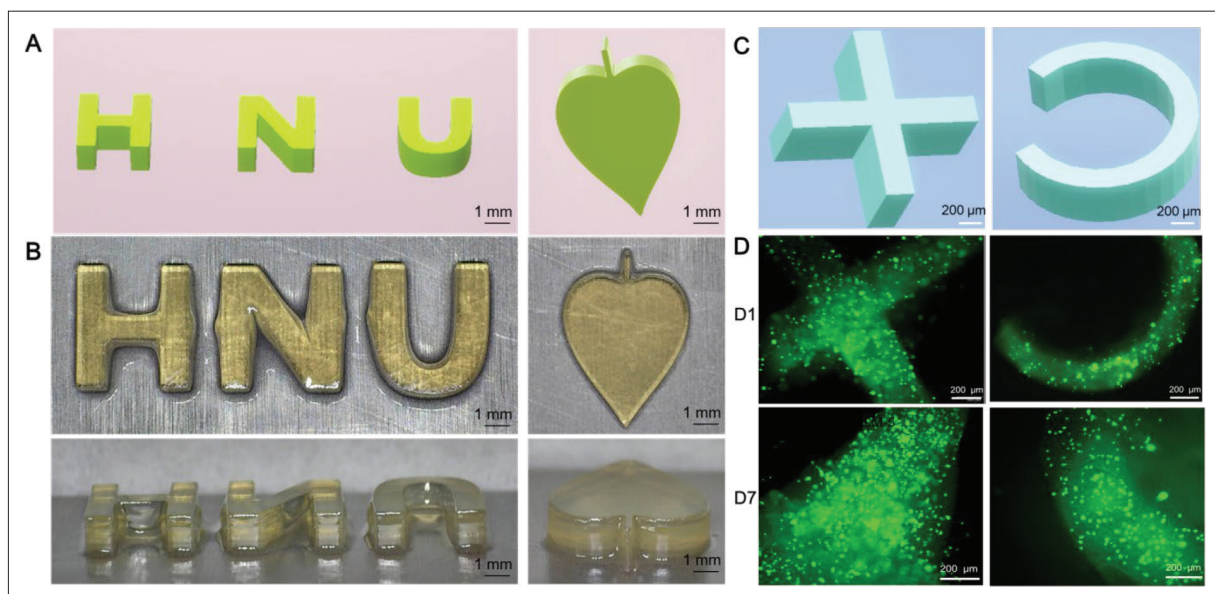


Figure 7. The 3D digital model (A and C) and printed constructs of the dSC-ECM-5 hydrogel by a DLP micro 3D printing system (B). Images of living chondrocytes encapsulated in dSC-ECM-5 after 7 days of culture by 3D bioprinting (D). Abbreviations: dSC-ECM-5, 5 mg dSC-ECMMA.

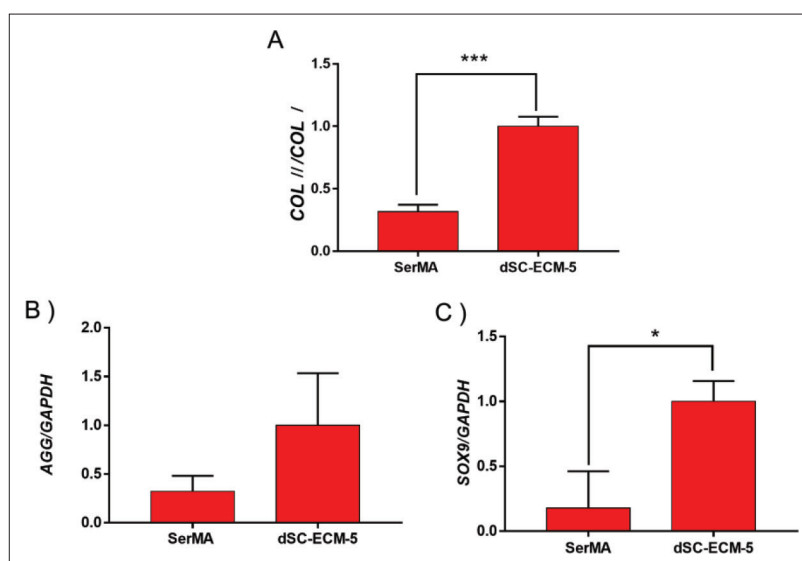


Figure 8. Transcription levels of the test genes in chondrocytes encapsulated in dSC-ECM-5 and SerMA hydrogels respectively *in situ* after 2 weeks of culture. (A) *COL II/COL I*, (B) *AGG*, (C) *SOX9*. (* $p < 0.05$, ** $p < 0.01$, *** $p < 0.001$, **** $p < 0.0001$). Abbreviations: dSC-ECM-5, 5 mg dSC-ECMMA; SerMa, sericin methacrylate.

to a clean culture dish, and incubated with cell culture medium for 1 and 7 days. Following 1-day incubation, samples were washed with ddH₂O and were applied with FDA staining to observe all living chondrocytes. It clearly displayed that living chondrocytes were evenly distributed all over the printed samples. After 7 days of incubation, encapsulated chondrocytes were alive, and a significantly increased number of them appeared, indicating that the proliferation of chondrocytes had been achieved in these printed products (Figure 7C and D). Taken together, it demonstrated that the dSC-ECM-derived bioink, dSC-ECM-5, is suitable for 3D bioprinting and tissue engineering applications.

3.6. The bioactive function of the dSC-ECM-5 bioink

To investigate whether the dSC-ECM-5 bioink influences the transcription of genes in chondrocytes, the transcription levels of the selected genes in chondrocytes, which were encapsulated in dSC-ECM-5 and SerMA hydrogels, respectively, were examined by RT-qPCR (Table 2). The transcription of type I collagen (*COL I*), type II collagen (*COL II*), aggrecan (*AGG*), and SRY-related HMG Box 9 (*SOX 9*) were chondrogenesis-related genes and were chosen to evaluate the influence of the dSC-ECM-5 bioink on cartilage regeneration. *SOX9* is an important transcription factor in chondrogenesis and is considered a key indicator of chondrocytic phenotype of chondrocytes. Compared to the SerMA bioink, the dSC-ECM-5 bioink significantly increased the transcription of *SOX9* (Figure 8) in chondrocytes, indicating that dSC-ECM-5 bioink may facilitate the formation of neocartilage

tissue. The ratio of mRNA *COL II/COL I* has been viewed as a crucial factor for chondrogenesis and the chondrocytic phenotype of chondrocytes^[28]. In contrast to the SerMA bioink, the *COL II/COL I* ratio is significantly improved by the dSC-ECM-5 bioink, indicating that chondrocytes in the dSC-ECM-5 hydrogels should be more efficient for cartilage regeneration. Hence, the dSC-ECM-5 bioink exhibited an additional function, which did not appear in the SerMA bioink and may promote cartilage regeneration.

3.7. The dSC-ECM-5 bioink enhances cartilage regeneration *in vivo*

Since evaluating tissue regeneration *in vivo* is the key criterion for determining whether a biomaterial is appropriate for tissue engineering^[29,30], solidified hydrogel samples, prepared with dSC-ECM-5 and SerMA bioinks containing chondrocytes respectively, were implanted into nude mice for 4 weeks. Following 4 weeks of implantation in mice, samples were collected and subjected to H&E staining, SO staining, and type II collagen immunohistochemical staining. Compared with the SerMA bioink, the dSC-ECM-5 bioink enhanced the cartilage-like tissue regeneration and promoted the new cartilage lacuna formation, demonstrating that the dSC-ECM-5 bioink is a promising bioink for cartilage tissue engineering applications. Moreover, the volume of cartilage-like tissue in specimens of the dSC-ECM-5 bioink was extremely larger than that of the SerMA bioink (Figure 9). It implied that the dSC-ECM-5 bioink significantly enhances the efficiency of cartilage tissue regeneration. In conclusion, the dSC-ECM-derived

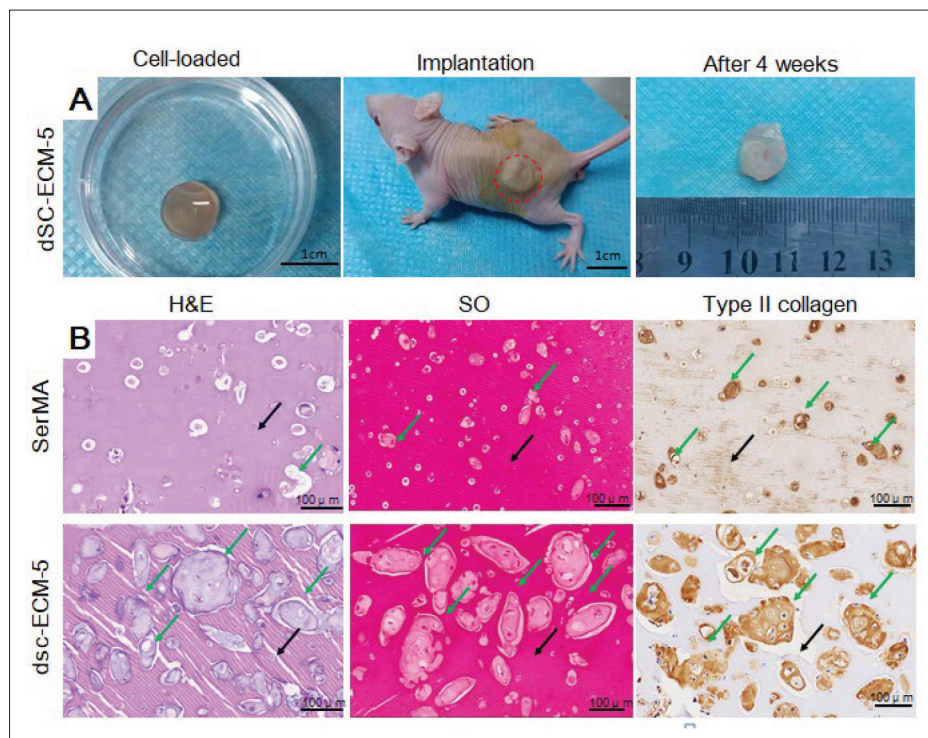


Figure 9. *In vivo* cartilage regeneration with samples prepared with dSC-ECM-5 and SerMA bioinks carrying chondrocytes, respectively. (A) Gross view; the photograph of nude mice after implantation with samples prepared with the dSC-ECM-5 bioink containing chondrocytes; the red circle indicates the sample. (B) Histological staining of H&E, SO, and type II collagen immunohistochemical staining of collected specimens following 4 weeks implantation in nude mice. Green arrows: new cartilage lacuna. Black arrows: residual hydrogel material. Abbreviations: dSC-ECM-5, 5 mg dSC-ECMMA; H&E, hematoxylin and eosin; SerMA, sericin methacrylate; SO, safranin-O.

bioink, the dSC-ECM-5 bioink, can be potential applied for cartilage tissue engineering application combined with 3D bioprinting in the future.

4. Discussion

The aim of this study is to set up a strategy, by which ECM-derived bioinks can be developed for organ engineering and tissue engineering via 3D bioprinting approach. Since an organ may be consisted of many different tissues, different ECM-derived bioinks should be required for achieving the goal of printing an organ or a tissue via 3D bioprinting. Theoretically, the cartilage tissue is composed of cartilage ECM and chondrocytes. It seems that a cartilage ECM-derived bioink may greatly facilitate the cartilage tissue engineering with 3D bioprinting tools. Considering the phenotype of chondrocytes plays a key role in cartilage tissue engineering, decellularized sturgeon cartilage ECM, which maintains the chondrocytic phenotype of chondrocytes, was selected as the target to develop a series of dSC-ECM-derived bioinks (Figure 1).

The dSC-ECM had been prepared successfully (Figure 2), and methacrylate-modified dSC-ECM was achieved as well (Figure 3). However, the dSC-ECMMA cannot totally

dissolve in water. The dSC-ECMMA aqueous solution is photo-curable, and its solidified hydrogel is hard and crisp (Figure S1). Then, to solve this problem, additional SerMA was added to dSC-ECMMA aqueous solution. Compared with SerMA hydrogels, the dSC-ECMMA hydrogels exhibited enhanced mechanical properties, which may benefit the tissue engineering applications (Figure S2). Based on these results, a series of dSC-ECM-derived bioinks, which contained the same SerMA and different weights of dSC-ECMMA, were prepared. These dSC-ECM-derived bioinks were named as dSC-ECM-5, dSC-ECM-10, and dSC-ECM-15, which contained 5mg/mL, 10mg/mL, and 15mg/mL dSC-ECMMA respectively. Interestingly, only the dSC-ECM-5 bioink allowed the proliferation of loaded chondrocytes compared with the SerMA bioink, suggesting that it should be selected for further tests (Figure 5). And photo-solidified dSC-ECMMA hydrogels showed a porous network, which allows nutrient transporting and cell migration (Figure 6).

The dSC-ECM-5 bioink is a promising bioink for 3D bioprinting, since the printed hydrogel products exhibited the high fidelity as designed shapes and displayed clearly outlines after bioprinting by applying it as the bioink

(Figure 7A and B). The printed products by using the dSC-ECM-5 bioink combined with 3D printer, were incubated with cell culture medium. Following 1 and 7 days of incubation, these encapsulated chondrocytes were alive and proliferated (Figure 7C and D). And the dSC-ECM-5 bioink influenced the transcription of chondrogenesis-related genes in chondrocytes, which were encapsulated in its solidified hydrogel. The dSC-ECM-5 hydrogel significantly elevated the mRNA level of SOX9 and improved COL III/COL I ratio, suggesting that it promotes the efficiency of cartilage regeneration and cartilage tissue maturation (Figure 8). To further confirm these *in vitro* results, samples produced with the dSC-ECM-5 and SerMA bioinks were, respectively, subcutaneous implanted into nude mice for 4 weeks. In consist with the *in vitro* data, the dSC-ECM-5 bioink significantly enhanced the efficiency of cartilage tissue regeneration and cartilage lacuna formation compared with the SerMA bioink (Figure 9). In summary, the dSC-ECM-derived bioink, the dSC-ECM-5 bioink, can be potentially used for the cartilage tissue engineering applications combined with 3D bioprinting approaches.

5. Conclusion

The dSC-ECM-derived bioink, the dSC-ECM-5 bioink, was fabricated by using dSC-ECMMA and SerMA. Solidified dSC-ECM-5 bioink exhibited good biocompatibility, reliable mechanical properties, and porous network, which are all required for tissue engineering applications. By applying the dSC-ECM-5 bioink combined with a proper 3D bioprinter, printed products display high fidelity as designed shapes and clear outlines, and allow encapsulated chondrocytes to proliferate. The dSC-ECM-5 bioink significantly enhanced the efficiency of cartilage regeneration and cartilage tissue maturation both *in vitro* and *in vivo*. Hence, the dSC-ECM-5 bioink can be a promising bioink for 3D bioprinting applications and potential applied for cartilage tissue engineering.

Acknowledgments

We thank Professor Rao Lang of Shenzhen Bay Laboratory for his support of the 3D printer.

Funding

The authors sincerely appreciate the supports of the National Key Research and Development Program of China [grant no. 2018YFC1105800], the Natural Science Foundation of Hunan Province [grant no. 2021JJ30095], and the Natural Science Foundation of Changsha City [grant no. kq2014040].

Conflict of interest

The authors declare no competing interests.

Author contributions

Conceptualization: Xiaolin Meng, Zheng Zhou, Hairong Liu

Investigation: Xiaolin Meng, Xin Chen, Wenxiang Zhu, Shuai Zhu

Methodology: Xiaolin Meng, Feng Ren

Software: Xin Chen, Feng Ren

Supervision: Zheng Zhou, Hairong Liu

Writing – original draft: Xiaolin Meng

Writing – review & editing: Zheng Zhou, Hairong Liu, Feng Ren

Ethics approval and consent to participate

The animal used has been reviewed and approved by the Institutional Animal Care and Use Committee (IACUC), The Second Xiangya Hospital, Central South University, China. The research ethics approval number is 2022006.

Consent for publication

Not applicable.

Availability of data

Not applicable.

References

1. Daly AC, Prendergast ME, Hughes AJ, *et al.*, 2021, Bioprinting for the biologist. *Cell*, 184(1):18–32.
<https://doi.org/10.1016/j.cell.2020.12.002>
2. Spencer AR, Shirzaei Sani E, Soucy JR, *et al.*, 2019, Bioprinting of a cell-laden conductive hydrogel composite. *ACS Appl Mater Interfaces*, 11(34):30518–30533.
<https://doi.org/10.1021/acsami.9b07353>
3. Chen N, Zhu K, Zhang YS, *et al.*, 2019, Hydrogel bioink with multilayered interfaces improves dispersibility of encapsulated cells in extrusion bioprinting. *ACS Appl Mater Interfaces*, 11(34):30585–30595.
<https://doi.org/10.1021/acsami.9b09782>
4. Yang H, Yang KH, Narayan RJ, *et al.*, 2021, Laser-based bioprinting for multilayer cell patterning in tissue engineering and cancer research. *Essays Biochem*, 65(3): 409–416.
<https://doi.org/10.1042/EBC20200093>
5. Moroni L, Burdick JA, Highley C, *et al.*, 2018, Biofabrication strategies for 3D in vitro models and regenerative medicine. *Nat Rev Mater*, 3(5):21–37.
<https://doi.org/10.1038/s41578-018-0006-y>

6. Valot L, Martinez J, Mehdi A, *et al.*, 2019, Chemical insights into bioinks for 3D printing. *Chem Soc Rev*, 48(15): 4049–4086.
<https://doi.org/10.1039/c7cs00718c>
7. Chimene D, Kaunas R, Gaharwar AK, 2020, Hydrogel bioink reinforcement for additive manufacturing: A focused review of emerging strategies. *Adv Mater*, 32(1):1902026.
<https://doi.org/10.1002/adma.201902026>
8. Ahlfeld T, Guduric V, Duin S, *et al.*, 2020, Methylcellulose: A versatile printing material that enables biofabrication of tissue equivalents with high shape fidelity. *Biomater Sci-UK*, 8(8):2102–2110.
<https://doi.org/10.1039/d0bm00027b>
9. Bandyopadhyay A, Ghosh S, Boccaccini AR, *et al.*, 2021, 3D printing of biomedical materials and devices. *J Mater Res*, 36(19):3713–3724.
<https://doi.org/10.1557/s43578-021-00407-y>
10. Oliveira EP, Malysz-Cymborska I, Golubczyk D, *et al.*, 2019, Advances in bioinks and in vivo imaging of biomaterials for CNS applications. *Acta Biomater*, 95: 60–72.
<https://doi.org/10.1016/j.actbio.2019.05.006>
11. Luo C, Xie R, Zhang J, *et al.*, 2020, Low-temperature three-dimensional printing of tissue cartilage engineered with gelatin methacrylamide. *Tissue Eng Part C Methods*, 26(6):306–316.
<https://doi.org/10.1089/ten.TEC.2020.0053>
12. Beck EC, Barragan M, Tadros MH, *et al.*, 2016, Approaching the compressive modulus of articular cartilage with a decellularized cartilage-based hydrogel. *Acta Biomater*, 38: 94–105.
<https://doi.org/10.1016/j.actbio.2016.04.019>
13. Masaeli E, Nasr-Esfahani MH, 2021, An in vivo evaluation of induced chondrogenesis by decellularized extracellular matrix particles. *J Biomed Mater Res A*, 109(5):627–636.
<https://doi.org/10.1002/jbm.a.37047>
14. Sun WY, Yang YY, Wang L, *et al.*, 2022, Utilization of an acellular cartilage matrix-based photocrosslinking hydrogel for tracheal cartilage regeneration and circumferential tracheal repair. *Adv Funct Mater*, 32(31):202201257.
<https://doi.org/10.1002/adfm>
15. Yang Z, Shi Y, Wei X, *et al.*, 2010, Fabrication and repair of cartilage defects with a novel acellular cartilage matrix scaffold. *Tissue Eng Part C Methods*, 16(5):865–876.
<https://doi.org/10.1089/ten.TEC.2009.0444>
16. Pati F, Jang J, Ha DH, *et al.*, 2014, Printing three-dimensional tissue analogues with decellularized extracellular matrix bioink. *Nat Commun*, 5: 3935.
<https://doi.org/10.1038/ncomms4935>
17. Bhattacharya R, Das P, Joardar SN, *et al.*, 2019, Novel decellularized animal conchal cartilage graft for application in human patient. *J Tissue Eng Regen Med*, 13(1):46–57.
<https://doi.org/10.1002/term.2767>
18. Das P, Singh YP, Joardar SN, *et al.*, 2019, Decellularized caprine conchal cartilage toward repair and regeneration of damaged cartilage. *ACS Appl Bio Mater*, 2(5):2037–2049.
<https://doi.org/10.1021/acsabm.9b00078>
19. Viegas CSB, Conceicao N, Fazenda C, *et al.*, 2010, Expression of Gla-rich protein (GRP) in newly developed cartilage-derived cell cultures from sturgeon (*Acipenser naccarii*). *J Appl Ichthyol*, 26(2):214–218.
<https://doi.org/10.1111/j.1439-0426.2010.01408.x>
20. Li Y, Chen W, Dai Y, *et al.*, 2021, Decellularized sturgeon cartilage extracellular matrix scaffold inhibits chondrocyte hypertrophy in vitro and in vivo. *J Tissue Eng Regen Med*, 15(8):732–744.
<https://doi.org/10.1002/term.3222>
21. Qi C, Liu J, Jin Y, *et al.*, 2018, Photo-crosslinkable, injectable sericin hydrogel as 3D biomimetic extracellular matrix for minimally invasive repairing cartilage. *Biomaterials*, 163: 89–104.
<https://doi.org/10.1016/j.biomaterials.2018.02.016>
22. Chen W, Xu Y, Li H, *et al.*, 2020, Tanshinone IIA delivery silk fibroin scaffolds significantly enhance articular cartilage defect repairing via promoting cartilage regeneration. *ACS Appl Mater Interfaces*, 12(19):21470–21480.
<https://doi.org/10.1021/acsami.0c03822>
23. Kim H, Kang B, Cui XL, *et al.*, 2021, Light-activated decellularized extracellular matrix-based bioinks for volumetric tissue analogs at the centimeter scale. *Adv Funct Mater*, 31(32).
<https://doi.org/10.1002/adfm.202011252>
24. Zhao H, He LY, 2022, Fabrication of neuroprotective silk-sericin hydrogel: Potential neuronal carrier for the treatment and care of ischemic stroke. *J Exp Nanosci*, 17(1):362–376.
<https://doi.org/10.1080/17458080.2022.2075545>
25. Xue H, Zhang ZH, Lin Z, *et al.*, 2022, Enhanced tissue regeneration through immunomodulation of angiogenesis and osteogenesis with a multifaceted nanohybrid modified bioactive scaffold. *Bioact Mater*, 18: 552–568.
<https://doi.org/10.1016/j.bioactmat.2022.05.023>
26. Huang Y, Meng X, Zhou Z, *et al.*, 2022, A naringin-derived bioink enhances the shape fidelity of 3D bioprinting and efficiency of cartilage defect repair. *J Mater Chem B*, 10(36):7030–7044.
<https://doi.org/10.1039/d2tb01247b>

27. Du Z, Li N, Hua Y, *et al.*, 2017, Physiological pH-dependent gelation for 3D printing based on the phase separation of gelatin and oxidized dextran. *Chem Commun (Camb)*, 53(97):13023–13026.
<https://doi.org/10.1039/c7cc08225h>
28. Bae M, Hwang D, Ko MK, *et al.*, 2021, Neural stem cell delivery using brain-derived tissue-specific bioink for recovering from traumatic brain injury. *Biofabrication*, 13(4):044110.
<https://doi.org/10.1088/1758-5090/ac293f>
29. Wei L, Qin S, Ye Y, *et al.*, 2022, Chondrogenic potential of manganese-loaded composite scaffold combined with chondrocytes for articular cartilage defect. *J Mater Sci Mater Med*, 33(10):74.
<https://doi.org/10.1007/s10856-022-06695-y>
30. Schuckert KH, Jopp S, Osadnik M, 2010, Modern bone regeneration instead of bone transplantation: A combination of recombinant human bone morphogenetic protein-2 and platelet-rich plasma for the vertical augmentation of the maxillary bone: A single case report. *Tissue Eng Part C Methods*, 16(6):1335–1346.
<https://doi.org/10.1089/ten.TEC.2010.0020>